Artur BERENDT[1], Jerzy MIZERACZYK[2], Janusz PODLIŃSKI[1]

The Szewalski Institute of Fluid Flow Machinery, Polish Academy of Sciences (1)
Gdynia Maritime University, Department of Marine Electronics (2)

doi:10.15199/48.2017.02.49

Electrostatic particle precipitation in a two-phase fluid in a needle-to-plate negative DC corona discharge

***Abstract**. In this paper we present instantaneous images of the electrohydrodynamic (EHD) smoke particle flow in air polluted with smoke, which illustrate the electrostatic particulate matter precipitation process in a needle-to-plate negative DC corona discharge in a two-phase fluid (air with particulate matter suspended in it) in the finite-volume discharge chamber. The recorded particle flow images show the temporal changes in the particle concentration in the discharge chamber during the transition of the two-phase EHD fluid (air and suspended particles) flow into the quasi single-phase EHD fluid flow (air). The instantaneous flow images enabled us to estimate the rate of electrostatic precipitation of the smoke particles.*

***Streszczenie.** W niniejszym artykule przedstawiono chwilowe zdjęcia elektrohydrodynamicznego (EHD) przepływu cząstek dymu w zapylonym powietrzu ilustrujące przebieg procesu elektrostatycznego odpylania w ujemnym wyładowaniu koronowym między elektrodami: igła-płyta w płynie dwufazowym (powietrze z zawieszonymi cząstkami pyłu) w zamkniętej komorze wyładowczej. Zarejestrowane chwilowe zdjęcie przepływu pokazują zmiany koncentracji cząstek dymu w komorze wyładowczej podczas przejście od przepływu w ośrodku dwufazowym (powietrze z zawieszonymi cząstkami dymu) do przepływu w ośrodku quasi-jednofazowym (powietrze). Chwilowe zdjęcia przepływu umożliwiły wyznaczenie szybkości elektrostatycznego usuwania cząstek dymu z komory wyładowczej. (**Elektrostatyczne odpylanie cząstek w przepływającym ośrodku dwufazowym wywołane ujemnym wyładowaniem koronowym w układzie elektrod igła-płyta**).*

Keywords: DC corona discharge, electrohydrodynamic flow, flow imaging, electrostatic precipitator, particulate matter precipitation
Słowa kluczowe: ujemne wyładowanie koronowe, przepływ elektrohydrodynamiczny, obrazowanie przepływu, elektrofiltr, elektrostatyczne usuwanie cząstek.

Introduction

When a strong electric field exists between a needle electrode and a plate electrode in a gaseous two-phase fluid (e.g. gas with the suspended particulate matter), a corona discharge occurs, first resulting in ionization of gas molecules and then, indirectly in charging the particulate matter. The existing electric field sets the gas molecules and particulates into motion, inducing the so-called electrohydrodynamic (EHD) two-phase fluid flow. [1]. The EHD flow induced in the flue gases by corona discharges has been used for almost hundred years for dust particle removal in electrostatic precipitators (ESPs) [2]. Despite of the one-hundred year history of electrostatic dust particle removal from two-phase fluids, there are scarce works on the inevitable transition of the two-phase fluid (e.g. air with suspended particles) into the single-phase fluid (air) in a corona discharge in the finite-volume chamber. Recently this subject has been tackled in [1]. The results of this paper clearly showed that such a phase transition exists in the negative corona in the finite-volume discharge chamber.

The experiment presented in this paper concerns the study of electrostatic precipitation of smoke particles suspended in air (both forming a two-phase fluid) in a finite-volume discharge chamber in which negative corona discharge between the needle-to-plate electrode arrangement was run. In particular, the process of the transition of the two-phase EHD fluid (air and the suspended smoke particles) into the quasi single-phase EHD fluid (air almost without the smoke particles), caused by the electrostatic removal of the smoke particles, is investigated. Such a study, as it will be shown, is useful for illustrating the mechanism of electrostatic particle removal from the gaseous two-phase fluid.

Experimental setup

The experimental apparatus (Fig. 1) for the study of particle precipitation in a gaseous two-phase fluid consisted of a discharge chamber with a needle-to-plate electrode arrangement inside, a high voltage supply, a high-voltage probe, an ammeter, a digital oscilloscope, a 2D TR PIV equipment and an aerosol spectrometer.

The discharge chamber was an acrylic box (L:W:H = 600 mm:120 mm: 50 mm). The needle-to-plate electrode arrangement was placed in it. The discharge chamber was filled with a gaseous two-phase fluid consisted of air with cigarette smoke particles suspended in it. The average diameter of cigarette smoke particles was about 0.3 μm (the size distribution of the cigarette smoke particles can be found in [3]). Before each measurement the discharge chamber was filled with "new" air having the smoke particles homogeneously distributed in it. The measuring has been started when the fluid was still in the chamber. The initial concentration of the particles was measured using the optical aerosol spectrometer GRIMM 1.109 (particles size scale ranging from 0.25 μm to 32 μm in 31 size channels).The initial concentration of the smoke particles was about 450 000 particles/cm^3.

The needle-to-plate electrode arrangement consisted of two electrodes, a needle and a plate. The needle electrode was made of a stainless-steel rod (1 mm in diameter), the end of which had a tapered profile with the tip having a radius of curvature of 75 μm. The plate electrode was also made of stainless-steel. The interelectrode gap was 25 mm. The negative high-voltage was applied to the needle electrode through a 3.3 MΩ resistor. The plate electrode was grounded.

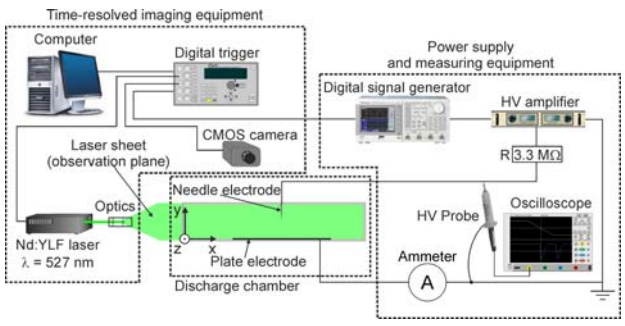

Fig.1. Experimental setup

The temporally-resolved imaging of the particle precipitation in the EHD two-phase fluid flow was carried out for a negative DC voltage. The negative DC voltage was

generated by a high-voltage power amplifier (Trek, 40/15), which amplified the voltage delivered by the function generator Tektronix AFG 3052C. The applied voltage amplitude was - 12 kV (measured between the needle electrode and the plate electrode using the high-voltage probe Tektronix, P6015A). The average corona discharge current was measured with the ammeter (Brymen, BM859CFa). The average corona discharge current changed with decreasing concentration of smoke particles, which have been continuously removed from the chamber volume due to the electrostatic particle precipitation. The corona current increased from about 15 μA at a particle concentration of 450 000 particles/cm^3 to about 21 μA when only traces of the smoke particles remained in the almost single-phase fluid (i.e. in the "smoke particle-free" air)

The temporally-resolved PIV system was used for both the flow imaging and the velocity vector field measurements. It consisted of a twin Nd:YLF laser (Litron, the wavelength of 527 nm, power laser pulse 30 mJ), imaging optics (cylindrical telescope), high speed CMOS camera (Phantom, Miro M310, camera sensor size of 1280 pixels × 800 pixels, acquisition rate of 3200 Hz at full frame), digital signal generator (BNC, 575) for triggering the function generator, laser pulses and camera shutter, computer for controlling the temporally-resolved PIV system, which recorded the captured images and performed digital analysis of the captured images. The smoke particles, which in principle formed the particulate matter phase were also employed as tracers in the PIV measurements. More detailed description of our temporally-resolved PIV system and measurement procedure can be found in [4].

The laser sheet plane (forming the observation plane) was fixed along the discharge chamber perpendicularly to the plate electrode, 1 mm from the axis of the needle electrode (z = −1 mm, Fig. 1). The instantaneous particle flow images were recorded for selected times after the negative corona inception, i.e. at times t = 1 s, t = 30 s, t = 60 s and t = 120 s. The repetition rate of the laser pulses in the pulse series was set at 3000 Hz (it means that the time between onsets of consecutive laser pulses was 0.33 ms). For a given times the series of 51 single laser pulses was launched and instantaneous particle flow images were recorded. Then 50 instantaneous velocity field maps were calculated. The EHD two-phase flow velocity field presented in this paper resulted from averaging of the 50 instantaneous velocity vector fields.

The instantaneous and time-averaged velocity vector fields were computed using Dantec DynamicStudio software. The interrogation area for the PIV cross-correlation procedure was 32 pixels x 32 pixels. The interrogation area overlap was 50%. The spatial resolution of determined time-averaged velocity vector fields was 1.6 mm × 1.6 mm.

Results

In our previous experiment [1] we studied mainly the temporal and spatial evolution of the EHD two-phase flow into the single-phase flow after the negative corona inception between the needle-to-plate electrode in the finite-volume chamber. The experiment in [1] was terminated 30 s after the corona inception, i.e. when the quasi single-phase fluid flow established. The experiment presented in this paper extends the observation time up to 120 s, which enables visual monitoring of the particle removal also in the final stage of the electrostatic precipitation of the particles in the finite-volume discharge chamber.

The images presented in Fig. 2 show the evolution of electrostatic precipitation of the suspended cigarette smoke particles in air after the corona inception (the time of the corona inception is taken as a reference time t = 0). These images are instantaneous maps of the laser light scattered by the suspended smoke particles in the observation plane formed by the laser beam. Thus, the white spots seen in the images are results of the laser light scattered by the smoke particles present in the fluid.

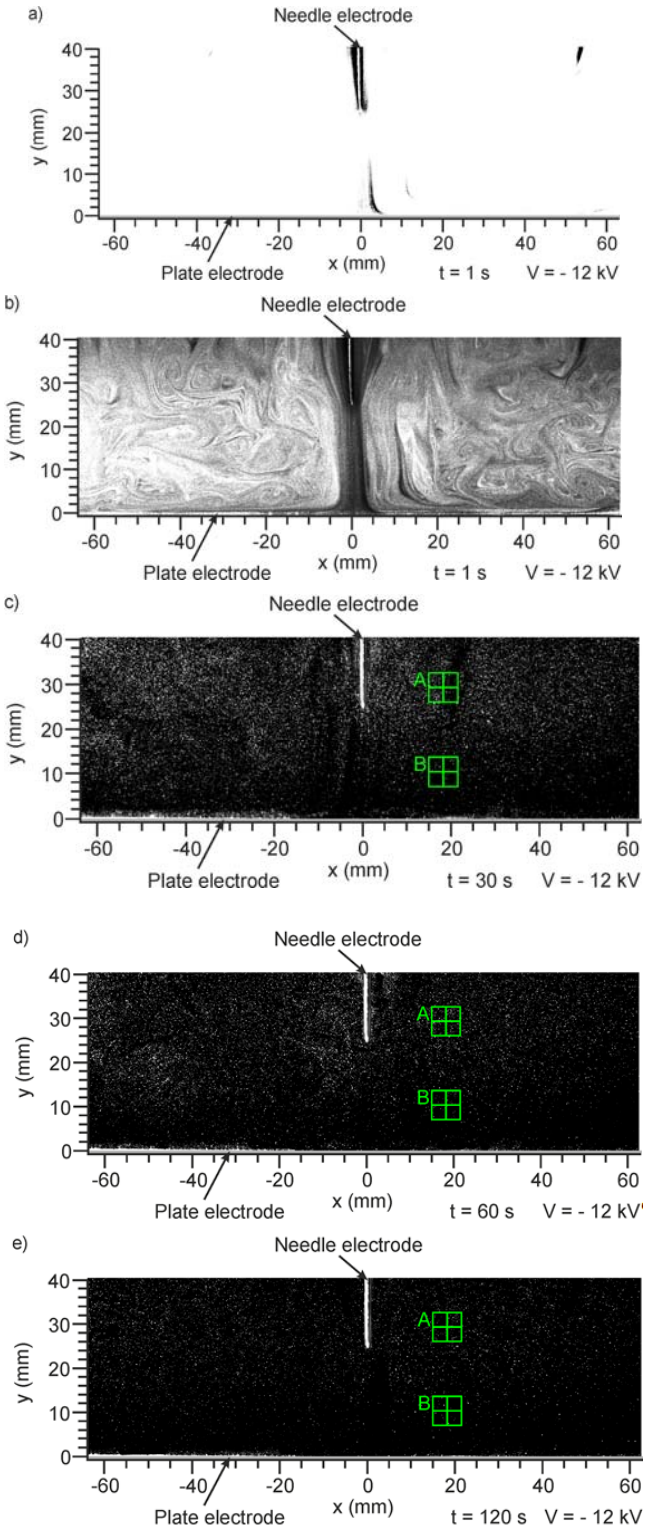

Fig.2. Imaging of particle precipitation process in the finite-volume discharge chamber. The initial concentration of smoke particles was 450 000 cm^{-3}. The images (a), (c), (d), (e) have the same greyscale. Note that the number of light spots (particles scattering laser light) gradually decrease in the subsequent images (c), (d) and (e)

The particle imaging in the discharge chamber was performed at times t = 1 s (Fig. 2a and 2b), t = 30 s (Fig. 2c), t = 60 s (Fig. 2d) and t = 120 s (Fig. 2e) after the corona inception. The images in Figs. 2a, 2c, 2d and 2e have the same greyscale. This preserves the relative light intensities (and information about the particles scattering the laser light) in all the images. However, the greyscale in Fig. 2b had been changed to show the particle flow details due to the overexposing of the image in Fig. 2a. Fig. 2a (t= 1 s) was taken when the concentration of the smoke particles was still high (about 450 000 cm^{-3}). As it can be seen the smoke particles scattered a lot of light and the image is overexposed (only needle electrode can be seen). By changing the grey scale, the fully developed two-phase EHD jet (the jet nomenclature taken from [5, 6]) between the needle and the plate electrode can be seen in Fig. 2b. The typical flow structure of this stage consists of a relatively wide cylindrical core (assuming 3D symmetry of the flow), coaxial with the needle electrode axis (more about evolution of EHD two-phase fluid flow in the needle-to-plate electrode arrangement can be found in [1, 4]).

In the images in Figs. 2c, 2d and 2e (images taken at times t = 30 s, 60 s and 120 s) the transition of the EHD two-phase fluid flow into the quasi single-phase fluid flow due to the electrostatic particle precipitation can be seen. These images show that most of smoke particles have been already precipitated. The particles that remained in the discharge chamber are seen as the separated light spots. As seen the remained particles are not homogeneously distributed in the discharge chamber. The number of particles near the plate electrode is smaller than that in the upper part of the discharge chamber. This can be clearly seen in Fig. 3.

Fig. 3 shows the blow-up of areas A and B marked in the images in Fig. 2 with green frames. Each area is divided into four smaller areas which size is 32 pixels x 32 pixels (3.175 mm x 3.175 mm), which corresponds to the interrogation area for the PIV cross-correlation procedure. It can be seen in the consecutive images in Figs. 3a (t = 30 s), 3b (t = 60 s), 3c (t = 120 s) that the number of smoke particles in A and B areas decrease with elapsing time.

The average numbers of smoke particles in the single interrogation area are as follows: at a time t = 30 s – in area A: 42, in area B: 15; at a time t = 60 s – in area A: 34, in area B: 11; and at a time t = 120 s – in area A: 15, in area B: 6. Thus, our above supposition that particles are not distributed homogeneously are confirmed. Such a smoke particles distribution seems to be intuitive because the electrostatic particle precipitation process takes place mainly near the plate electrode (especially around the axis of the needle electrode). The other walls of the discharge chamber (made of the electric isolator) do not participate in the particle collection).

Besides, Fig. 4 shows that also the EHD flow (in the finite-volume chamber) influences the particles distribution. Fig. 4 presents the time-averaged velocity vector field of the EHD particle flow measured at a time t = 60 s. As seen the EHD flow pushes the particles present near the needle electrode axis towards the plate electrode. Majority of the charged particles are collected on the plate electrode, while the rest of them and those uncharged are pushed along the plate. In the vicinity of the discharge chamber walls, made of the isolator, the EHD flow lifts up the particles to the upper part of discharge chamber (not shown in this paper). As a result, the particle concentration in the upper part of the discharge chamber becomes higher than that near the plate electrode, as it can be seen in images in Fig. 2.

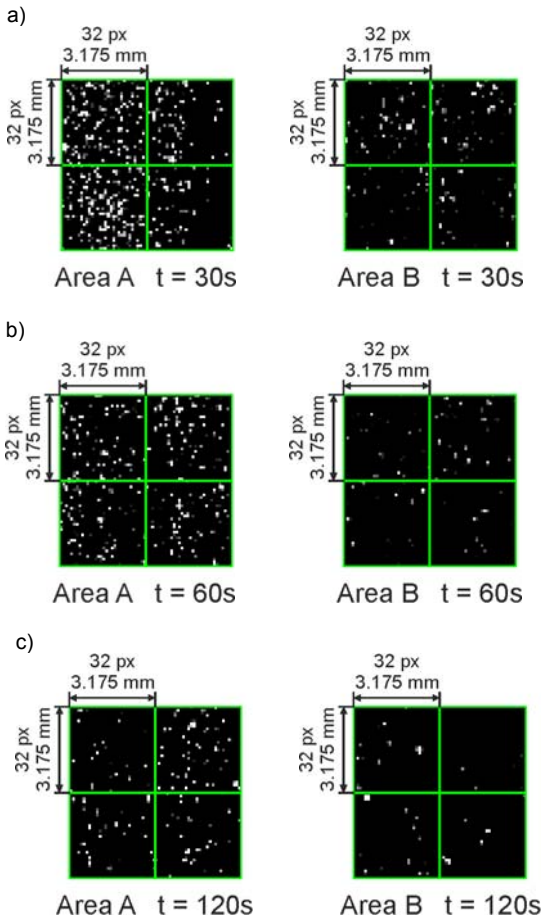

Fig.3. Blow-up of areas A and B marked in the images presented in Fig. 2

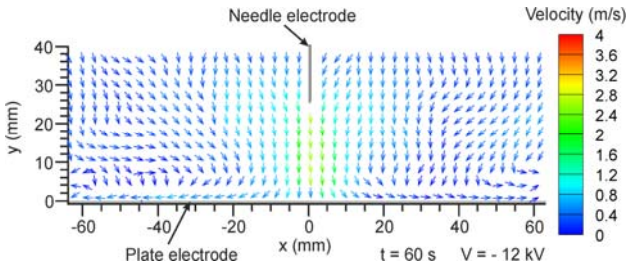

Fig.4. Time-averaged velocity vector field map of the EHD particle flow

Knowing the average number of smoke particles in the interrogation area (3.175 mm x 3.175 mm) from Fig. 3 and the thickness of the laser sheet (about 2 mm) makes the approximate calculation of the smoke particle concentration in the discharge chamber at times t = 30 s, 60 s and 120 s possible. Fig. 5 shows the time dependence of the smoke particle concentration C(t) in the discharge chamber in natural logarithm-linear scale. Startlingly the particle concentration time-dependence in the natural logarithm-linear scale may be approximated with two lines that have different slopes. This means that the particle concentration time-dependence can be approximated with two e^{-kt} functions in which k is the particle precipitation rate in s^{-1}. Fig. 5 shows that shortly after the corona inception particle concentration decreased rapidly, i.e. it dropped from the initial concentration of 450 000 cm^{-3} to 1440 cm^{-3} within a time t = 0 - 30 s, which corresponds to the particle removal rate k_1 = 0.191 s^{-1}. After a time of t = 30 s the particle precipitation process was much slower. The particle

concentration at a time t = 60 s and t = 120 s was 1140 cm^{-3} and 545 cm^{-3}, respectively. This gives the particle rate k_2 = 0.025 s^{-1} within a time range t = 30 - 120 s (i.e. k_2 is about 7.6 times smaller than k_1). In other words, the particle precipitation rate is about 19.1 % s^{-1} in the first participation period (0 - 30 s) and then it drops to about 2.5 % s^{-1}. It seems that the precipitation rate change have the following reason. The probability that the smoke particle will be in the precipitation zone was very high when the particle concentration in the discharge chamber was high, i.e. in the period short after the corona inception. Thus, in the first precipitation period the precipitation rate k_1 was high. When the particle concentration in the discharge chamber dropped (after a time t = 30 s), it was less likely that the smoke particle will be present in the precipitation zone. Therefore, the particle precipitation rate k_2 was smaller than the k_1.

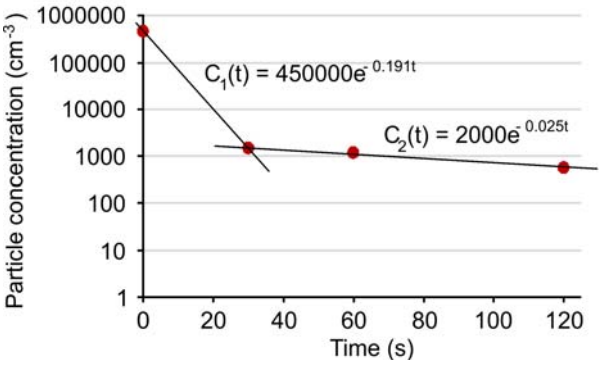

Fig.5. The smoke particle concentration C(t) in the discharge chamber versus time

Summary

The results of the presented experiment are as follows. The captured instantaneous EHD flow images of smoke particles in air illustrated the process of the electrostatic particle precipitation in the two-phase EHD fluid (air with suspended smoke particles) in the needle-to-plate negative DC corona discharge in the finite-volume chamber. The images showed clearly the transition of the two-phase EHD fluid flow (air and smoke particles) into the quasi single-phase EHD fluid (air) flow. The vector velocity field maps obtained with the PIV method showed the influence of the EHD flow on the distribution of smoke particles in the discharge chamber in the final precipitation stage.

We found that shortly after the corona inception, i.e. in the first participation stage (0 - 30 s, when the particle concentration was relatively high) the particle concentration decreased rapidly. In this stage the particle precipitation rate was k_1 = 0.191 s^{-1}. In the second precipitation stage (within a time range t = 30 - 120 s, when the particle concentration was low) the particle precipitation rate was k_2 = 0.025 s^{-1}. This means that the particle precipitation rate k_2 was about 7.6 times smaller than k_1. The moment when the particle precipitation rate changes from k_1 to k_2 corresponds with the moment of the transition from the two-phase EHD fluid to the quasi single-phase EHD fluid. This suggests that time-fluctuations of the dust particle concentration in the flue gas flow in ESP may result in the corresponding variation of the dust particle precipitation rate.

This work was supported by the National Science Centre (grant UMO-2013/09/B/ST8/02054).

***Authors**: mgr Artur Berendt, Instytut Maszyn Przepływowych im. Roberta Szewalskiego Polskiej Akademii Nauk, Ośrodek Techniki Plazmowej i Laserowej, ul. Fiszera 14, 80-231 Gdańsk, E-mail: aberendt@imp.gda.pl; prof. dr hab. inż. Jerzy Mizeraczyk, Akademia Morska w Gdyni, Wydział Elektryczny, Katedra Elektroniki Morskiej, ul. Morska 81-87, 81-225 Gdynia, E-mail: jmiz@imp.gda.pl; dr inż. Janusz Podliński, Instytut Maszyn Przepływowych im. Roberta Szewalskiego Polskiej Akademii Nauk, Ośrodek Techniki Plazmowej i Laserowej, ul. Fiszera 14, 80-231 Gdańsk, E-mail: janusz@imp.gda.pl.*

REFERENCES

[1] Berendt A., Mizeraczyk J., Transition of the electrohydrodynamic two-phase flow into the single-phase flow in a needle-to-plate negative corona discharge in the finite-volume chamber, J. Electrostat., 84 (2016), 90-96

[2] Mizuno A., Electrostatic precipitation, IEEE Trans. Dielectr. Electr. Insul. 7 (2000), No. 5, 615-624

[3] Sahu, S.K, Tiwari M., Bhangare R.C., Pandit G.G., Particle Size Distribution of Mainstream and Exhaled Cigarette Smoke and Predictive Deposition in Human Respiratory Tract, Aerosol Air Qual. Res., 13 (2013), 324-332

[4] Mizeraczyk J., Berendt A, Podliński J., Temporal and spatial evolution of EHD particle flow onset in air in a needle-to-plate negative DC corona discharge, J. Phys. D: Appl. Phys., 49 (2016), 205203

[5] Yu J., Vuorinen V., Hillamo H., Sarjovaara T., Kaario O., Larmi M., An experimental investigation on the flow structure and mixture formation of low pressure ratio wall-impinging jets by a natural gas injector, J. Nat. Gas Sci. Eng., 9 (2012), 1-10

[6] Zuckerman N., Lior N., Jet impingement heat transfer: physics, correlations, and numerical modeling, Adv. Heat Transfer, 39 (2006), 565-631